Infection, Genetics and Evolution 90 (2021) 104762

Contents lists available at ScienceDirect

Infection, Genetics and Evolution

journal homepage: www.elsevier.com/locate/meegid

Short communication

# Genomic evolution of avian polyomaviruses with a focus on budgerigar fledgling disease virus

Eszter Kaszab [a], Szilvia Marton [a], Károly Erdélyi [b], Krisztián Bányai [a], Enikő Fehér [a,*]

[a] Institute for Veterinary Medical Research, Centre for Agricultural Research, Hungária krt. 21, Budapest H-1143, Hungary
[b] National Food Chain Safety Office, Tábornok utca 2, Budapest H-1143, Hungary

ARTICLE INFO

*Keywords:*
Avian polyomavirus
Budgerigar fledgling disease virus
Viral evolution

ABSTRACT

Gammapolyomaviruses may cause serious inflammatory diseases in a broad range of avian hosts. In this study we investigated genomic evolution of and selection constraint acting on avian polyomaviruses (APyVs). Our analyses suggested that goose haemorrhagic polyomavirus (GHPV) evolves more slowly ($3.03 \times 10^{-5}$ s/s/y mean evolutionary rate) than budgerigar fledgling disease virus (BFDV), finch polyomavirus (FPyV) and canary polyomavirus (CaPyV) ($1.39 \times 10^{-4}$ s/s/y, $2.63 \times 10^{-4}$ s/s/y and $1.41 \times 10^{-4}$ s/s/y mean evolutionary rate, respectively). In general, purifying selection seems to act on the protein coding regions of APyV genomes, although positive Darwinian selection was also predicted in a few positions (e.g., in the large tumor antigen coding region of BFDV and GHPV and in the capsid protein sequences of BFDV). The importance of these aa changes remains elusive. Overall, a better understanding of adaptive changes in the genome of APyVs requires additional data from various incidental hosts and reservoir species.

Avian polyomaviruses (APyVs) are unique among polyomaviruses in that they may induce serious inflammatory diseases in their natural hosts (Johne and Müller, 2007). For example, haemorrhagic nephritis and enteritis of geese caused by the goose haemorrhagic polyomavirus (GHPV) and the French molt associated with the budgerigar fledgling disease virus (BFDV), respectively, have been well known diseases of domesticated geese and pet birds for decades (Bernáth and Szalai, 1970; Bernier et al., 1981; Bozeman et al., 1981; Johne and Müller, 2007; Phalen et al., 1997). Adult hosts may shed APyVs directly through feces and feathers horizontally to their nestlings and mates, but contaminated environment may be a source of infection as well (Palya et al., 2004; Phalen et al., 1997). Infected birds may show poor condition, weight loss and feather disorders, accompanied by gross pathological changes, e.g. swelling of internal organs, and haemorrhages in the skin and the gastrointestinal tract. Neurological signs before sudden death of infected young birds is seen quite often (Bernáth and Szalai, 1970; Bernier et al., 1981; Bozeman et al., 1981; Johne and Müller, 2007; Palya et al., 2004; Phalen et al., 1997). Persistent and subclinical infections are common in adult birds that may help maintain the transmission chain of APyVs (Kaszab et al., 2020; Palya et al., 2004; Phalen et al., 1997).

Polyomaviruses of birds are classified into nine species within the *Gammapolyomavirus* genus and the *Polyomaviridae* family; these are *Anser anser polyomavirus 1* (goose haemorrhagic polyomavirus, GHPV), *Aves polyomavirus 1* (budgerigar fledgling disease virus, BFDV), *Corvus monedula polyomavirus 1* (crow polyomavirus), *Cracticus torquatus polyomavirus 1* (butcherbird polyomavirus), *Erythrura gouldiae polyomavirus 1*, *Lonchura maja polyomavirus 1* (Hungarian finch polyomavirus), *Pygoscelis adeliae polyomavirus 1* (Adélie penguin polyomavirus), *Pyrrhula pyrrhula polyomavirus 1* (finch polyomavirus, FPyV) and *Serinus canaria polyomavirus 1* (canary polyomavirus, CaPyV) (Calvignac-Spencer et al., 2016; Circella et al., 2017; Marton et al., 2016). The length of gammapolyomaviral dsDNA genomes falls between 4971 and 5422 bp. In each case the genome contains the ORFs of the VP1, VP2 and VP3 viral proteins as well as the large and small T antigens (LTA and STA, respectively) (Johne and Müller, 2007). The genome of GHPV, FPyV, crow polyomavirus, butcherbird polyomavirus, *Erythrura gouldiae polyomavirus 1*, and Hungarian finch polyomavirus was predicted to encode the ORF-X that, despite the high nt and aa difference, may have functional similarities with the VP4 of BFDV (Johne and Müller, 2007).

Sequence data revealed that highly similar strains of BFDV, GHPV,

*Abbreviations:* APyVs, avian polyomaviruses;; BFDV, budgerigar fledgling disease virus;; CaPyV, canary polyomavirus;; FPyV, finch polyomavirus;; GHPV, goose haemorrhagic polyomavirus;; LTA, large T antigen;; STA, small T antigen;; VP1-VP4, viral protein 1–4.

* Corresponding author.
*E-mail address:* feher.eniko@atk.hu (E. Fehér).

https://doi.org/10.1016/j.meegid.2021.104762
Received 7 January 2021; Received in revised form 4 February 2021; Accepted 5 February 2021
Available online 8 February 2021
1567-1348/© 2021 The Authors. Published by Elsevier B.V. This is an open access article under the CC BY-NC-ND license (http://creativecommons.org/licenses/by-nc-nd/4.0/).

CaPyV and FPyV may infect variable avian hosts (Circella et al., 2017; Johne and Müller, 2007; Kaszab et al., 2020; Li et al., 2019; Styś-Fijoł et al., 2016). In this research project we aimed at exploring the diversity of various avian polyomaviruses, and to reveal the genomic diversity and the evolution of BFDV. A recently identified BFDV strain from Hungary was added to the analyses. To put the findings in a broader context of avian polyomavirus evolution, we systematically collected available genomic sequences of other gammapolyomaviruses from GenBank and performed additional calculations. These data included genomic sequences of GHPV, FPyV and CaPyV.

With respect to the BFDV sequence generated for the present study we used previously published methods (Kaszab et al., 2020). In brief, BFDV infection was diagnosed with the nested PCR primer sets VP1-1f and Vp1-1r, and Vp1-2f and Vp1-2r as described by Johne et al. (2005) from a mixture of liver and kidney samples of a juvenile ring-necked parakeet (*Psittacula krameri*). The bird had a history of quick weight loss and succumbed within a few days from the onset of diseases in an aviary in 2011, Hungary. Macroscopically the bird exhibited signs of general circulatory collapse, congestion of all internal organs, splenomegaly, hepatomegaly and swollen kidneys. Histology revealed multifocal haemorrhages in the liver, kidneys, spleen and heart, acute multifocal necrotic hepatitis, multifocal tubular necrosis in the kidneys and follicular depletion in the spleen.

The complete genome of the identified BFDV strain was amplified by two sets of back-to-back PCR primers (bPyVbbF1 5'-ACGCTATTTCAG-TATCCAGCTG-3′ and bPyVbbR1 5'-GGTAGGCCTCGCCAATATTG-3′; bPyVbbF2 5′- TGTATCTGGTTTGCTAAACTCCTTG-3′ and bPyVbbR2 5'-GGATAGGGGTTACGAACATTACG-3′) in PCR mixtures containing 200 nM of primers, 200 μM dNTP mix, 1× Phusion Green buffer, 0.3 U Phusion DNA Polymerase (Thermo Fisher Scientific), and 1 μl of nucleic acid extracted with DNeasy Blood & Tissue kit (Qiagen). The cycling protocol included a denaturation step at 98 °C for 30 s, followed by 40 cycles with the steps of 98 °C for 10 s, 54 °C for 30 s and 72 °C for 2.5 min, and a final extension step at 72 °C for 10 min. The amplicons were purified from agarose gel (Geneaid Gel/PCR DNA Fragments Extraction Kit) followed by library preparation and sequencing using the Ion Torrent PGM platform separately for both PCR product. The sequencing workflow was identical to that described elsewhere (Kaszab et al., 2020). The BFDV genome was assembled with the CLC Genomics Workbench software v7. The de novo assembled genome sequence of the BFDV strain 14525 (GenBank acc.no. MN657184) was 4981 bp long, and consisted of ORFs encoding the proteins typical for BFDVs, including the LTA (1800 nt), STA (438 nt), VP1 (1032 nt),-VP2 (1026 nt), VP3 (708 nt), VP4 (531 nt) and VP4d (339 nt) (Johne and Müller, 2007). BLAST analysis of the novel BFDV sequence showed 99.3–99.8% genome-wide nt identity with BFDV sequences available in the GenBank. The nt and translated aa sequence identities were ≤ 100% when comparing the individual genes of strain 14525 to reference BFDV sequences (Fig. 1).

The BFDV ($n = 27$; GenBank accession numbers are shown in Fig. 1), FPyV ($n = 5$; GenBank acc. no. KY986576–578, KC660158, DQ192571) and CaPyV ($n = 6$, GenBank acc. no. KY986579–583, GU345044) sequences were aligned using the AliView software (Larsson, 2014). Phylogenetic relationships among the BFDV sequences were investigated with the PhyML software, using the best fitting GTR + G model (Guindon et al., 2010). Recombination analysis of the sequence alignments was performed with the RDP4 software (Martin et al., 2015). Phylogenetic trees were generated from the alignments with the IQ-TREE online tool (Trifinopoulos et al., 2016) and the temporal structure was investigated with the TempEst v1.5.3 software to see if the sequence data set was suitable for additional evolutionary analysis (Rambaut et al., 2016). Evolutionary rates (given as substitutions per nucleotide site per year, s/s/y) were estimated using the Bayesian Markov chain Monte Carlo method of the BEAST package 1.10.4 with the best fit substitution models after evaluation of various models as implemented in the PhyML software (Table 1) (Lefort et al., 2017; Suchard et al., 2018). After initial testing of the data set using various test parameters, the sequences finally were analysed with uncorrelated log normal relaxed molecular clock, constant size coalescent tree prior and 50 million of iterations (sampling every 1000 steps). The effective sample size and evolutionary rates were checked with Tracer v1.7 (Rambaut et al., 2018). Maximum clade credibility tree was generated with FigTree v1.4.2 (http://tree.bio.ed.ac.uk/software/figtree). Selection constraint and the ratio of non-synonymous to synonymous mutations (dN/dS) were calculated with the fixed effect likelihood (FEL), the fast unconstrained Bayesian approximation for inferring selection (FUBAR) and mixed effects model of evolution (MEME) methods of the Datamonkey server (Weaver et al., 2018). Regarding GHPV, corresponding data were extracted from our previous study (Kaszab et al., 2020).

Prior to evolutionary analyses, the BFDV, FPyV and CaPyV sequence alignments were subjected to recombination detection analysis, but evidence for recombination was not found in the data sets. The sequence data showed positive correlation (the correlation coefficient ranged between 0.6134 and 0.7744 for complete genome sequences, and 0.1878–0.8623 for individual gene data sets) between the collection date and genetic divergence as determined with the TempEst software.

Regarding BFDV, phylogenetic inference of complete genome sequences permitted the resolution of two genetic lineages separated in 1964 (95% HPD interval 1931–1982) (Fig. 1). One lineage contained a sequence from Germany, collected in 1982, and two sequences from Germany and Mozambique, collected in 1995. This lineage did not include any strains from subsequent years. The other lineage split into two main branches. A single sequence, identified in Japan in 1982, represented the first branch that separated from the other in 1975 that comprised sequences described between 2003 and 2018. As seen for the maximum likelihood and time-scaled phylogenetic tree as well, the Hungarian BFDV sequence clustered with sequences originating from samples of other parakeets (including all of the the ring-necked parakeets), collected in Poland and China between 2009 and 2011, and with the sequence of a BFDV strain identified in pigeon (*Columba livia domestica*) sample collected in China in 2018 (Fig. 1). BFDV was also diagnosed in fecal samples of pigeons in a Chinese aviary that showed feather disorders (Li et al., 2019). The appearance of highly similar BFDV strains in psittacines and non-psittacine birds indicates broad host-range, a finding that emphasizes the need for precautions during bird transport, handling and keeping in order to avoid virus transmission among susceptible specimens of various host species.

Evolutionary rates were estimated for complete genomes and for each gene of BFDVs. Next, whenever possible, data were compared with that of other APyVs. The effective sample size was >200 for the investigated parameters of the used data sets. In brief, BFDV showed nearly ten times higher evolutionary rate (mean, $1.39 \times 10^{-4}$ s/s/y, 95% HPD $7.18 \times 10^{-5}$ - $2.10 \times 10^{-4}$) than that calculated for GHPV (31 analysed sequences, $3.03 \times 10^{-5}$ s/s/y, 95% HPD $1.09 \times 10^{-5}$ - $5.33 \times 10^{-5}$, Kaszab et al., 2020) but was similar when compared with the evolutionary rate of FPyV (mean, $2.63 \times 10^{-4}$ s/s/y, 95% HPD $1.60 \times 10^{-8}$ - $6.26 \times 10^{-4}$) and of CaPyV (mean, $1.41 \times 10^{-4}$ s/s/y, 95% HPD $5.75 \times 10^{-10}$ - $7.17 \times 10^{-4}$) (Table 1). The evolutionary rates ranged between $7.03 \times 10^{-5}$ and $2.28 \times 10^{-4}$ s/s/y for the individual gene sets of the BFDV with the fastest evolving genomic region occupied by the VP1-VP3 genes. Similar rates were calculated for FPyV, but those were lower for the gene equivalents when analysing the counterparts in the GHPV genomes (see Table 1 for details) (Kaszab et al., 2020). We would note, that less support was obtained for confidence intervals of estimated evolutionary rates in data sets containing fewer nt substitutions (e.g. for GHPV) or limited sample size (e.g. for FPyV and CaPyV).

In general, purifying selection seems to act on most of the genes of APyVs and a low number of sites under selective pressure were detected (Table 1, Fig. 2). However, nt and aa changes were found often in single sequences that may be the consequence of processes other than those driven by a particular selection constraint. Of note is that the limited

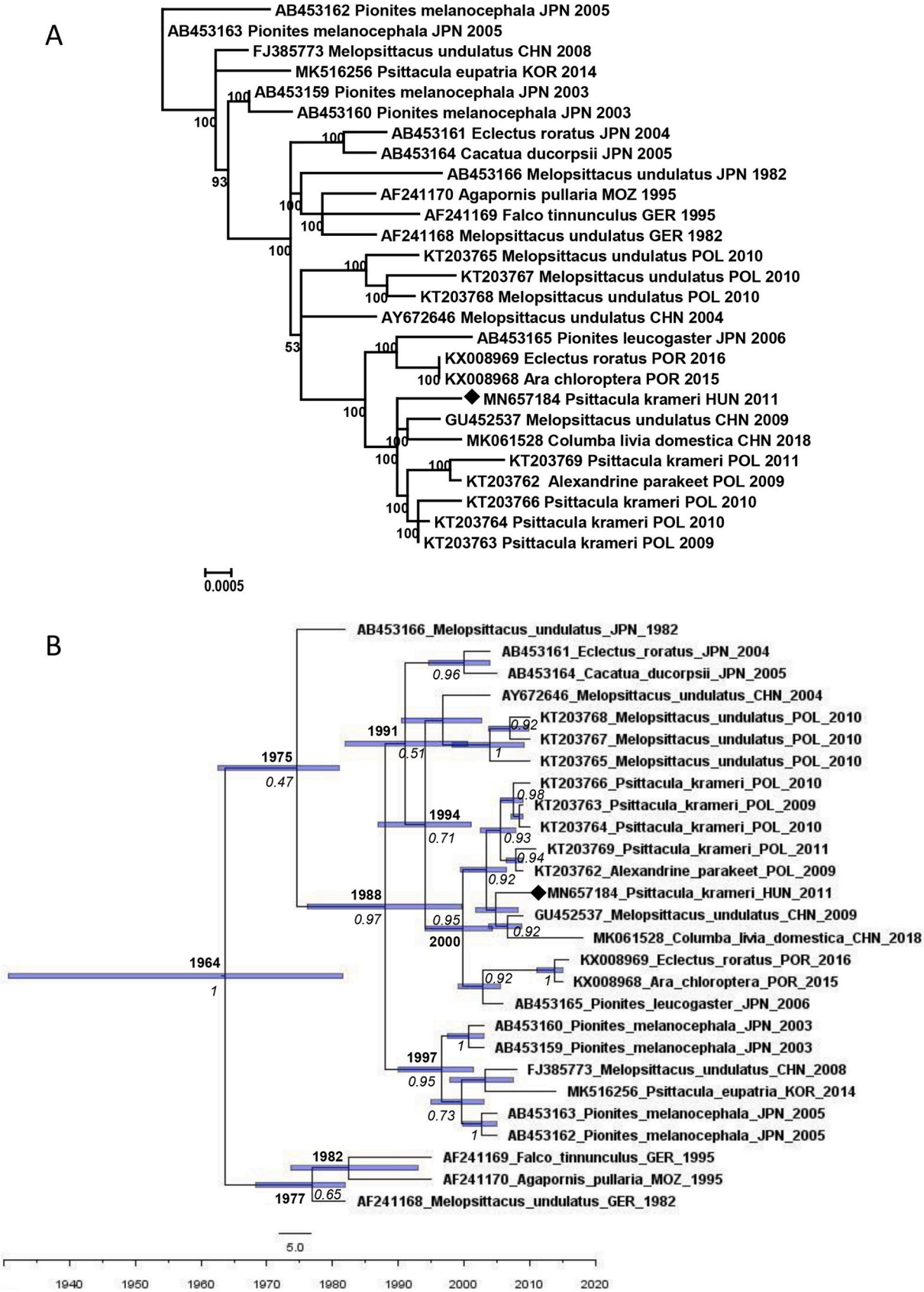


**Fig. 1.** (A) Maximum likelihood phylogenetic tree of budgerigar fledgling disease polyomavirus complete genome sequences using the GTR + G model of the PhyML software. The scale bar represents nucleotide substitutions per site. (B) Time-calibrated maximum clade credibility tree of budgerigar fledgling disease polyomavirus complete genome sequences. 95% highest posterior density intervals for the node ages are indicated with blue bars. Posterior probabilities at nodes are written with italic type. The strain collected in Hungary is labelled with black rectangle.

**Table 1**
The mean evolutionary rates and dN/dS ratios estimated for the complete genome and individual gene sequences of budgerigar fledgling disease virus (BFDV), goose haemorrhagic polyomavirus (GHPV) (Kaszab et al., 2020) and finch polyomavirus (FPyV).

| GHPV | | | | BFDV | | | | FPyV | | | |
|---|---|---|---|---|---|---|---|---|---|---|---|
| Gene | Evol. rate model | Evol. rate | dN/dS | Gene | Evol. rate model | Evol. rate | dN/dS | Gene | Evol. rate model | Evol. rate | dN/dS |
| **VP1** | HKY + G + I | **$4.82 \times 10^{-5}$** ($1.03 \times 10^{-8}$ - $1.24 \times 10^{-4}$) | 0.111 | **VP1** | JC | **$1.58 \times 10^{-4}$** ($7.88 \times 10^{-5}$ - $2.45 \times 10^{-4}$) | 0.322 | **VP1** | JC | **$2.00 \times 10^{-4}$** ($4.40 \times 10^{-6}$ - $4.77 \times 10^{-4}$) | 0.038 |
| **VP2** | HKY | **$1.25 \times 10^{-5}$** ($6.76 \times 10^{-12}$ - $5.46 \times 10^{-5}$) | 0.194 | **VP2** | JC + G | **$1.78 \times 10^{-4}$** ($8.93 \times 10^{-5}$ - $2.74 \times 10^{-4}$) | 0.798 | **VP2** | JC | **$1.452 \times 10^{-4}$** ($2.45 \times 10^{-6}$- $3.59 \times 10^{-4}$) | 0.110 |
| **VP3** | HKY | **$6.57 \times 10^{-6}$** ($5.27 \times 10^{-13}$ - $3.38 \times 10^{-5}$) | 0.644 | **VP3** | JC + G | **$2.28 \times 10^{-4}$** ($1.11 \times 10^{-4}$ - $3.60 \times 10^{-4}$) | 0.702 | **VP3** | JC | **$1.84 \times 10^{-4}$** ($3.03 \times 10^{-6}$ - $4.61 \times 10^{-4}$) | 0.160 |
| **LTA** | HKY + G | **$4.87 \times 10^{-5}$** ($4.39 \times 10^{-6}$ - $1.00 \times 10^{-4}$) | 0.0916 | **LTA** | JC + G | **$8.02 \times 10^{-5}$** ($3.63 \times 10^{-5}$ - $1.30 \times 10^{-4}$) | 0.156 | **LTA** | JC | **$2.931 \times 10^{-4}$** ($1.28 \times 10^{-5}$ - $6.53 \times 10^{-4}$) | 0.180 |
| **STA** | HKY + G | **$5.82 \times 10^{-5}$** ($3{,}05 \times 10^{-10}$ - $1.37 \times 10^{-4}$) | 0.111 | **STA** | JC | **$1.55 \times 10^{-4}$** ($6.19 \times 10^{-5}$ - $2.62 \times 10^{-4}$) | 0.0547 | **STA** | JC | **$2.28 \times 10^{-4}$** ($2.72 \times 10^{-6}$ - $5.96 \times 10^{-4}$) | 0.270 |
| **ORF-X** | HKY | **$2.98 \times 10^{-5}$** ($1.73 \times 10^{-9}$ - $8.53 \times 10^{-5}$) | 0.963 | **VP4** | JC | **$9.64 \times 10^{-5}$** ($3.41 \times 10^{-5}$ - $1.69 \times 10^{-4}$) | 0.720 | **ORF-X** | JC | **$3.214 \times 10^{-4}$** ($5.60 \times 10^{-6}$ - $7.77 \times 10^{-4}$) | 0.264 |
| **–** | – | – | – | **VP4d** | JC | **$7.03 \times 10^{-5}$** ($1.29 \times 10^{-5}$ - $1.39 \times 10^{-4}$) | 1.430 | **–** | – | – | – |
| **genome** | HKY + G + I | **$3.03 \times 10^{-5}$** ($1.09 \times 10^{-5}$ - $5.33 \times 10^{-5}$) | – | **genome** | JC + G | **$1.39 \times 10^{-4}$** ($7.18 \times 10^{-5}$ - $2.10 \times 10^{-4}$) | – | **genome** | JC | **$2.63 \times 10^{-4}$** ($1.60 \times 10^{-8}$ - $6.26 \times 10^{-4}$) | – |

The mean evolutionary rates are estimated as substitutions per sites per year (s/s/y); 95% HPD (highest posterior density) intervals are shown in parentheses.

number of available genome sequences from various host species may distort analysis results we obtained. The distribution and amount of sites under negative and positive selection pressure differed for all studied APyV species (Fig. 2). GHPV seems to have a slightly more conservative genome compared to BFDV and FPyV, whereas the low variability of CaPyV strains did not allow selection analysis to be performed.

The dN/dS ratio ranged between 0.0547 and 1.43 for the genes of BFDV. These values were higher than that estimated for FPyV (0.038–0.270), except for the STA gene (Table 1). Regarding GHPV, the STA and ORF-X showed slightly higher dN/dS ratio compared to the STA and VP4 of BFDV, respectively. The highest dN/dS ratios were calculated for the VP4d of BFDV (1.43) and the ORF-X of GHPV (0.963) that was consistent with neutral selection effect (Kaszab et al., 2020). VP4 is a structural component of BFDV that facilitates packaging of the viral genome (Johne and Müller, 2001; Johne et al., 2007). Furthermore, its splicing variant (with deletion of aa 68–131 of the VP4), the VP4d protein induces apoptosis of the infected cells; thus it may contribute to viral pathogenesis (Johne and Müller, 2001; Johne et al., 2007). Based on sequence comparisons, the ORF-X of GHPV was predicted to have functions similar to the VP4/VP4d of BFDV (Johne and Müller, 2007). The significance of the identified non-synonymous mutations in these regions is unknown. Although, compared to other genes, the dN/dS ratio was higher in the VP4d of BFDV and ORF-X of GHPV, the applied calculation methods did not highlight statistically any sites under diversifying selection (Fig. 2).

Positive selection acting on aa site 65, 173, 205 and 325 in the major capsid protein (VP1) of BFDV was identified with a combination of predictive tools, but these changes were present in single sequences (Fig. 2). Regarding the minor capsid proteins, most of the non-synonymous mutations accumulated in the central part of the VP2 (24/33 nt and 17/21 aa substitution sites) and within-frame overlapping VP3 (24/28 nt and 17/17 aa substitution sites) genes of BFDV (Fig. 2). The FUBAR software statistically supported diversifying selection acting on two sites (aa 221 and aa 240 of the VP2, and aa 115 and aa 134 of the VP3, respectively) of these genes (Fig. 2). The VP1-VP3 proteins are components of the viral capsid, thus aa changes expressed on these proteins may have a role in immune escape or may influence virulence of the virus. Statistically relevant positively selected sites were not detected for the VP1-VP3 of GHPV and FPyV (Kaszab et al., 2020).

The differences in the length and aa motifs of the LTA of avian and mammalian polyomaviruses and the scant experimental results make comparisons difficult for this genomic region (Johne and Müller, 2007). Thus, the significance of the selection pressure affecting single sites in the BFDV and GHPV LTA (at aa 575 and 100, respectively) (Fig. 2) cannot be ascertained. Regarding the STA, only few sites under negative selection pressure were denoted (Fig. 2).

The estimation of evolutionary rates revealed slightly faster evolution of BFDV and FPyV in comparison with GHPV. However, the calculations were based on a relatively narrow dataset. Adaptation to various hosts may promote accumulation of non-synonymous nt substitutions in the viral genome, thus investigation of sequence sets with a broad range of host species may show inflated s/s/y values in a relatively short sampling timeframe (Aiewsakun and Katzourakis, 2016). This may be true for all investigated BFDV strains and other gammapolyomaviruses (Kaszab et al., 2020). Other factors, e.g. the spatio-temporal distribution of the investigated virus strains and the measured subpopulations of the virus may influence the evolutionary and selection constraint calculations (Aiewsakun and Katzourakis, 2016).

The significance of polyomavirus infection identified in avian hosts, in which polyomavirus was not detected previously, needs to be elucidated. At present, few genomic sequences are available for most of the gammapolyomaviruses that made our objectives somewhat difficult to accomplish; collection of polyomavirus sequence data from samples of diverse bird species is needed to provide more precise picture on the host range of any particular gammapolyomavirus species and place evolutionary analyses on a more solid basis.

## Ethics approval

The authors confirm that no ethical approval was required. This work was carried out with diagnostic samples and no animal experimentation was conducted.

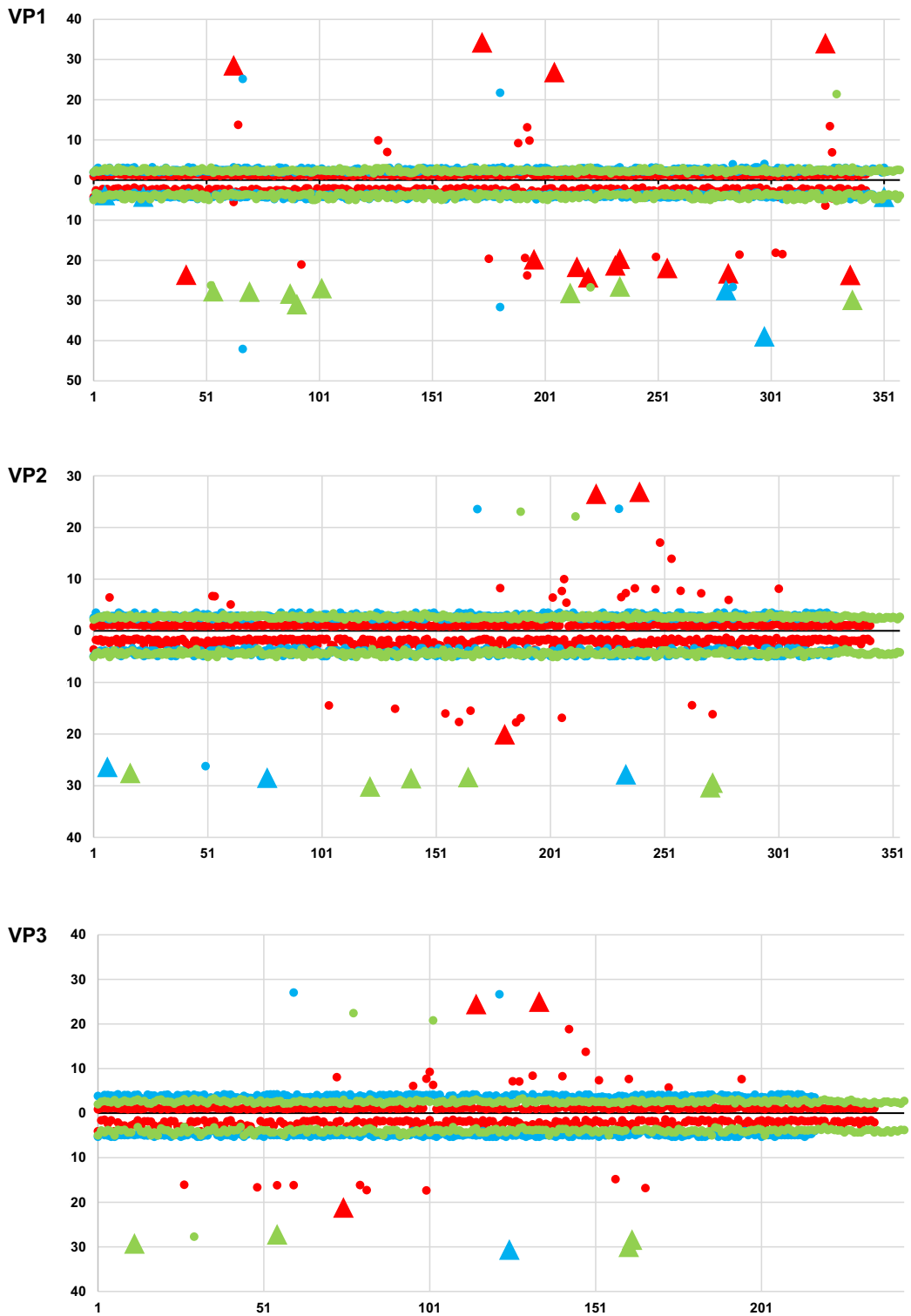


**Fig. 2.** Representation of β (mean posterior non-synonymous substitution rate at a site, y-axis above the x-axis) and α (mean posterior synonymous substitution rate at a site, y-axis below the x-axis) values extracted from FUBAR analyses of budgerigar fledgling disease virus (red), goose haemorrhagic polyomavirus (blue) and finch polyomavirus (green) genes. Statistically relevant values (with posterior probability of 0.9) are highlighted with triangles.

## Availability of data and material

The sequence data are available in the GenBank with accession number MN657184.

## Author contributions

K.B. and E.F. designed the study. K.E. provided samples and data. E. K., S.M., K.B. and E.F. performed experiments and data analysis. E.K., K. B. and E.F. prepared the first manuscript draft. All authors read and

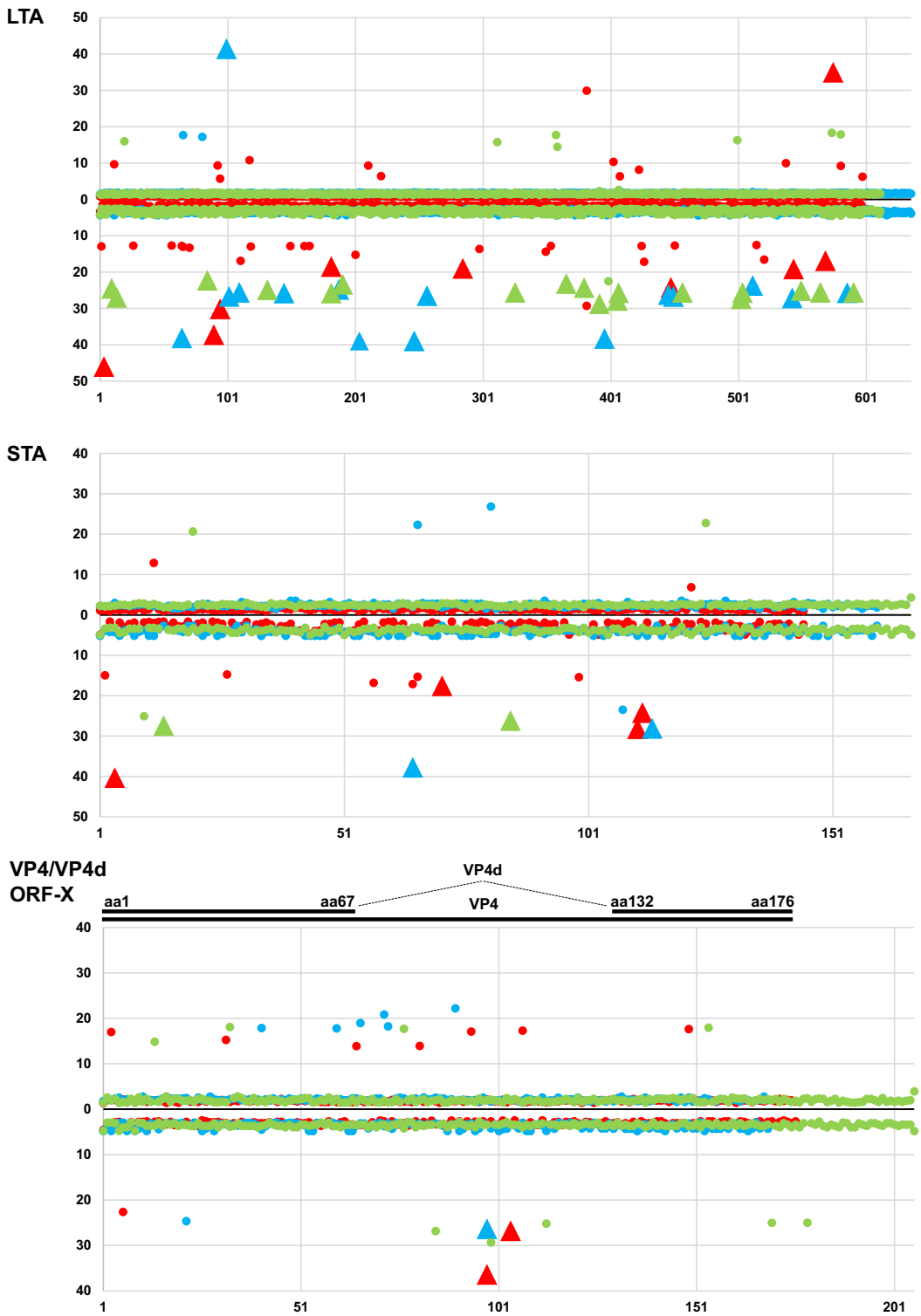


**Fig. 2.** (*continued*).

approved the manuscript.

## Declaration of competing interest

The authors declare no conflict of interest.

## Acknowledgements

The work was supported by the National Research, Development and Innovation Office (NKFI-OTKA, PD115519 – EF, and K120201 - KB). EF and SM were supported by the Bolyai János Fellowship program awarded by the Hungarian Academy of Sciences.

## References


Aiewsakun, P., Katzourakis, A., 2016. Time-dependent rate phenomenon in viruses. J. Virol. 90 (16), 7184–7195. https://doi.org/10.1128/JVI.00593-16.

Bernáth, S., Szalai, F., 1970. Investigation for clearing the etiology of the disease appeared among goslings in 1969 (in Hungarian). Magyar Állatorvosok Lapja. 25, 531–536.

Bernier, G., Morin, M., Marsolais, G., 1981. A generalized inclusion body disease in the budgerigar (*Melopsittacus undulatus*) caused by a papovavirus-like agent. Avian Dis. 25 (4), 1083–1092.

Bozeman, L.H., Davis, R.B., Gaudry, D., Lukert, P.D., Fletcher, O.J., Dykstra, M.J., 1981. Characterization of a papovavirus isolated from fledgling budgerigars. Avian Dis. 25 (4), 972–980.

Calvignac-Spencer, S., Feltkamp, M.C., Daugherty, M.D., Moens, U., Ramqvist, T., Johne, R., Ehlers, B., 2016. A taxonomy update for the family Polyomaviridae. Arch. Virol. 161 (6), 1739–1750. https://doi.org/10.1007/s00705-016-2794-y.

Circella, E., Caroli, A., Marino, M., Legretto, M., Pugliese, N., Bozzo, G., Cocciolo, G., Dibari, D., Camarda, A., 2017. Polyomavirus infection in Gouldian finches (Erythrura gouldiae) and other pet birds of the family Estrildidae. J. Comp. Pathol. 156 (4), 436–439. https://doi.org/10.1016/j.jcpa.2017.01.006.

Guindon, S., Dufayard, J.F., Lefort, V., Anisimova, M., Hordijk, W., Gascuel, O., 2010. New algorithms and methods to estimate maximum-likelihood phylogenies: assessing the performance of PhyML 3.0. Syst. Biol. 59 (3), 307–321. https://doi.org/10.1093/sysbio/syq010.

Johne, R., Müller, H., 2001. Avian polyomavirus agnoprotein 1a is incorporated into the virus particle as a fourth structural protein, VP4. J. Gen. Virol. 82, 909–918. https://doi.org/10.1099/0022-1317-82-4-909.

Johne, R., Müller, H., 2007. Polyomaviruses of birds: etiologic agents of inflammatory diseases in a tumor virus family. J. Virol. 81 (21), 11554–11559. https://doi.org/10.1128/JVI.01178-07.

Johne, R., Enderlein, D., Nieper, H., Müller, H., 2005. Novel polyomavirus detected in the feces of a chimpanzee by nested broad-spectrum PCR. J. Virol. 79 (6), 3883–3887. https://doi.org/10.1128/JVI.79.6.3883-3887.2005.

Johne, R., Paul, G., Enderlein, D., Stahl, T., Grund, C., Müller, H., 2007. Avian polyomavirus mutants with deletions in the VP4-encoding region show deficiencies in capsid assembly and virus release, and have reduced infectivity in chicken. J. Gen. Virol. 88, 823–830. https://doi.org/10.1099/vir.0.82506-0.

Kaszab, E., Marton, S., Dán, Á., Farsang, A., Bálint, Á., Bányai, K., Fehér, E., 2020. Molecular epidemiology and phylodynamics of goose haemorrhagic polyomavirus. Transbound. Emerg. Dis. 67 (6), 2602–2608. https://doi.org/10.1111/tbed.13608.

Larsson, A., 2014. AliView: a fast and lightweight alignment viewer and editor for large datasets. Bioinformatics. 30, 3276–3278. https://doi.org/10.1093/bioinformatics/btu531.

Lefort, V., Longueville, J.E., Gascuel, O., 2017. SMS: smart model selection in PhyML. Mol. Biol. Evol. 34 (9), 2422–2424. https://doi.org/10.1093/molbev/msx149.

Li, Q., Niu, K., Sun, H., Xia, Y., Sun, S., Li, J., Wang, F., Feng, Y., Peng, X., Zhu, L., Fan, X., Qin, Y., Ding, J., Jiang, H., Xu, G., 2019. Complete genome sequence of an avian polyomavirus strain first isolated from a pigeon in China. Microbiol. Resour. Announc. 8 (10) https://doi.org/10.1128/MRA.01490-18 e01490–18.

Martin, D.P., Murrell, B., Golden, M., Khoosal, A., Muhire, B., 2015. RDP4: detection and analysis of recombination patterns in virus genomes. Virus Evol. 1 (1) https://doi.org/10.1093/ve/vev003 vev003.

Marton, S., Erdélyi, K., Dán, Á., Bányai, K., Fehér, E., 2016. Complete genome sequence of a variant Pyrrhula pyrrhula polyomavirus 1 strain isolated from white-headed Munia (Lonchura maja). Genome Announc. 4 (6) https://doi.org/10.1128/genomeA.01172-16 e01172–16.

Palya, V., Ivanics, E., Glávits, R., Dán, A., Mató, T., Zarka, P., 2004. Epizootic occurrence of haemorrhagic nephritis enteritis virus infection of geese. Avian Pathol. 33 (2), 244–250. https://doi.org/10.1080/0307945042000195740.

Phalen, D.N., Wilson, V.G., Graham, D.L., 1997. Prevalence of neutralizing antibody and virus shedding in psittacine birds infected with avian polyomavirus. J. Avian Med. Surg. 11 (2), 98–104.

Rambaut, A., Lam, T.T., Carvalho, L.M., Pybus, O.G., 2016. Exploring the temporal structure of heterochronous sequences using TempEst. Virus Evol. 2 https://doi.org/10.1093/ve/vew007 vew007.

Rambaut, A., Drummond, A.J., Xie, D., Baele, G., Suchard, M.A., 2018. Posterior summarisation in Bayesian phylogenetics using tracer 1.7. Syst. Biol. 67, 901–904. https://doi.org/10.1093/sysbio/syy032.

Styś-Fijoł, N., Kozdruń, W., Czekaj, H., 2016. Preliminary survey of the occurrence of goose haemorrhagic polyomavirus (GHPV) in wild birds in Poland. J. Vet. Res. 60, 135–139. https://doi.org/10.1515/jvetres-2016-0019.

Suchard, M.A., Lemey, P., Baele, G., Ayres, D.L., Drummond, A.J., Rambaut, A., 2018. Bayesian phylogenetic and phylodynamic data integration using BEAST 1.10. Virus Evol. 4 https://doi.org/10.1093/ve/vey016 vey016.

Trifinopoulos, J., Nguyen, L.T., von Haeseler, A., Minh, B.Q., 2016. W-IQ-TREE: a fast online phylogenetic tool for maximum likelihood analysis. Nucleic Acids Res. 44 (W1), W232–W235. https://doi.org/10.1093/nar/gkw256.

Weaver, S., Shank, S.D., Spielman, S.J., Li, M., Muse, S.V., Pond, S.L.K., 2018. Datamonkey 2.0: a modern web application for characterizing selective and other evolutionary processes. Mol. Biol. Evol. 35 (3), 773–777. https://doi.org/10.1093/molbev/msx335.